

Enhanced Microfluidics Mixing Performance in a Grooved Serpentine Microchannel at Different Flow Rates

Faruk Aksoy^{1,2} , Gurkan Yesiloz^{1,2*} 

¹National Nanotechnology Research Center (UNAM) - Bilkent University, Çankaya-Ankara, Türkiye

²Institute of Material Science and Nanotechnology, Bilkent University, Çankaya-Ankara, Türkiye

*gurkan@unam.bilkent.edu.tr

*Orcid No: 0000-0002-1769-8201

Received: 06 May 2023

Accepted: 04 September 2023

DOI: 10.18466/cbayarfbe.1293522

Abstract

Reliable and efficient mixing in microfluidic systems is crucial for various applications such as molecular diagnostics, DNA hybridization, microreactors and nanoparticle synthesis. However, achieving adequate mixing at the microscale is challenging due to the fact that flow regime in microfluidics is laminar that is characterized by low Reynolds numbers. In an attempt to tackle this challenge, active and passive strategies have been utilized to enhance mixing. Passive techniques mainly rely on the interaction between fluid and channel geometry in order to extend the interface between the components of the fluid by inducing transversal flows. Passive methods have shown their simplicity over the active methods in microfluidics by simply controlling the channel geometry and flow configurations without involving any complex external forces and components. Based on this, our work presents a passive micromixer design with trapezoidal grooves placed at the bottom of the serpentine channels. The grooves induce periodic pressure drops along the channel which create staggered transversal vortices in orthogonal directions which disturbs the symmetries in the flow that results in stirring. These combined effects result in an enhanced mixing performance especially at higher flow rates. The results suggest that the design could be integrated into lab-on-a-chip systems to achieve enhanced mixing of biological or chemical components with reduced footprint, complexity and cost.

Keywords: Microfluidics; passive micromixers; grooved serpentine channels; mixing index; enhanced microfluidic mixing; computational fluid dynamics

1. Introduction

Lab-on-a-chip systems and microfluidic devices are extensively used in biological and chemical sciences [1,2] for various applications spanning from the synthesis of colloidal systems and nanoparticles (NPs) [3,4] to cell biology [5] and molecular diagnostics [6,7], owing to their ability to spatially control liquid composition with cellular resolution [8], reduced consumption of reactants [9], and the better control over reaction variables such as the reactant concentration and temperature [10]. Ideally, the utilization of these devices in biological assays/bioengineering and chemical analysis requires them to be capable of efficiently mixing predictably two or more biological or chemical components [11]. Thus, mixing element is one of the most critical and a fundamental building block in the development of microfluidic systems. However, it is also one of the

difficult functionalities to achieve because the length scales involved in microfluidics force a laminar flow regime that is characterized by low Reynolds numbers.

A number of research activities on this subject is continued to be carried out in order to achieve efficient mixing at the microscale. The employed methods, reported in the literature, to enhance mixing in laminar flow, diffusion-dominated, microscale regimes, are classified as either active or passive. Active techniques incorporate external actuators with the micromixer design in order to add an external force on the fluids in an effort to enhance mass transport within the micromixer and mix the unmixed inhomogeneous fluid solution [12]. Even though these strategies have proven to have good mixing capabilities, it comes at the price of more complex designs that are harder to integrate into analysis systems, and expensive scale-up.

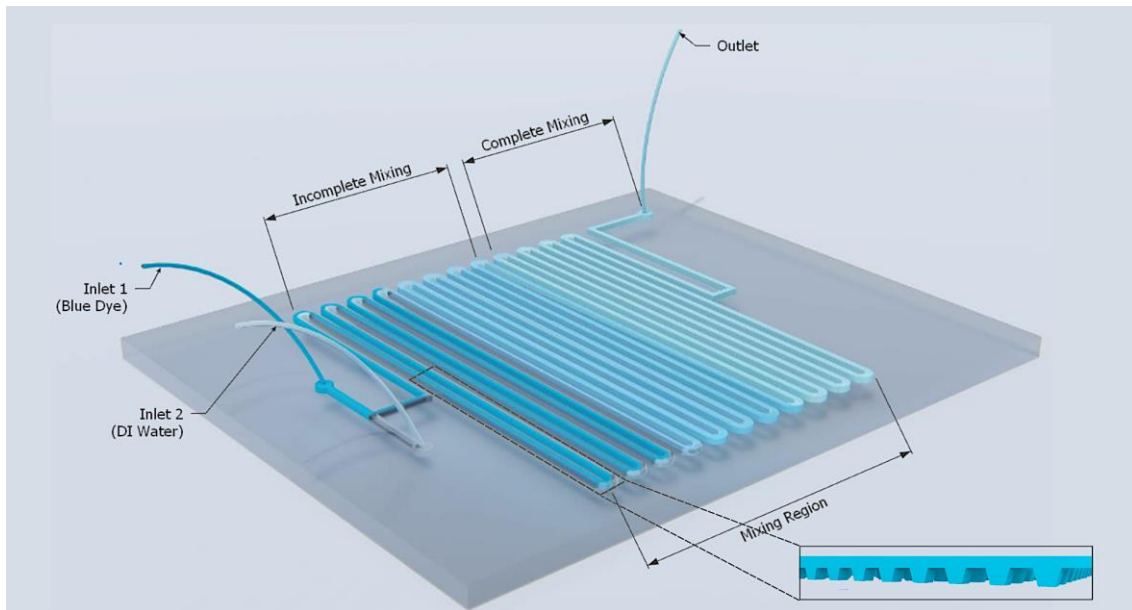


Figure 1. Schematic of the developed grooved serpentine microchannels for enhanced mixing.

Passive strategies, on the other hand, rely on the interactions between fluid and channel geometry. Such enhanced interactions induce transversal flows that stretch the interface between the fluids components to be mixed, and cause advection and/or breaking the symmetries in the flow [13].

In literature, numerous studies have been reported about enhancing mixing using passive techniques. The reported methods mainly rely on either chaotic and lamination advection-based designs [14-19], or utilized geometric manipulations to induce chaotic advection [20-27]. However, such passive designs that integrate obstacles/microstructure to disrupt fluid and increase mass transport, can impose very high localized strains which is capable of damaging biomolecules due to generated high shear stresses. Serpentine-based mixers have proven to prevent this damage because chaotic advection, due to high local strains, does not occur in these channels [28]. The centrifugal forces exerted by the curvy edges of the serpentine on the fluid, i.e., Dean flow, are accountable for this privilege. However, simple serpentine channels require longer footprint to achieve complete and homogeneous mixing, and usually causing inefficient mixing at higher flow rates.

Based on this, the proposed design investigated in this work involves a comparison in mixing performance between a simple serpentine micromixer and a grooved serpentine micromixer composed of 3D-trapezoidal grooves aligned to the bottom side of the microchannel. The current study takes the advantage of the fact that grooves induce staggered transversal vortices that are vertical for the grooves and horizontal for the main serpentine channel making two flows in orthogonal directions coupled with the Dean flow induced streamlines due to the serpentine itself.

Thus, an amplified transport of mass between the fluids which results in an enhanced mixing efficiency.

2. Materials and Methods

2.1. Experimental Setup and Fabrication

The experimental setup consists of two microfluidic chips integrated with a fluid pumping unit (Syringe pumps, Rotalab NE-4000), and an inverted microscope (Zeiss, Axio Observer 7) equipped with a CCD camera. The schematic of the developed microfluidic mixer unit is demonstrated in Figure 1.

2.1.1. Chip Fabrication

Soft lithography and 3D printing techniques are used to fabricate the proposed microfluidic chip. Briefly, after the master fabrication, 10:1 ratio of polydimethylsiloxane (PDMS) to curing agent is prepared, mixed and poured onto two masters; one containing the simple serpentine and other containing the grooves design separately. After curing the PDMS at 65° C on hot plate for 2 hrs PDMS is peeled off followed by the bonding of the simple serpentine with the grooves with fine alignment under microscope after oxygen plasma treatment. The final design is then bonded into a glass slide after oxygen plasma treatment. Fabrication is finished by a post baking of the chip at 45° C for 2 hrs.

2.1.2. PDMS Surface Treatment

After chip fabrication, a PDMS surface treatment is done to remove any possibility of air bubbles. For this, the microchannel is flushed with a chemical composition containing 1:2 of TEOS to ethanol (v/v). The solution is left for 5 minutes for incubation. Later, the chip is washed with Deionized water.

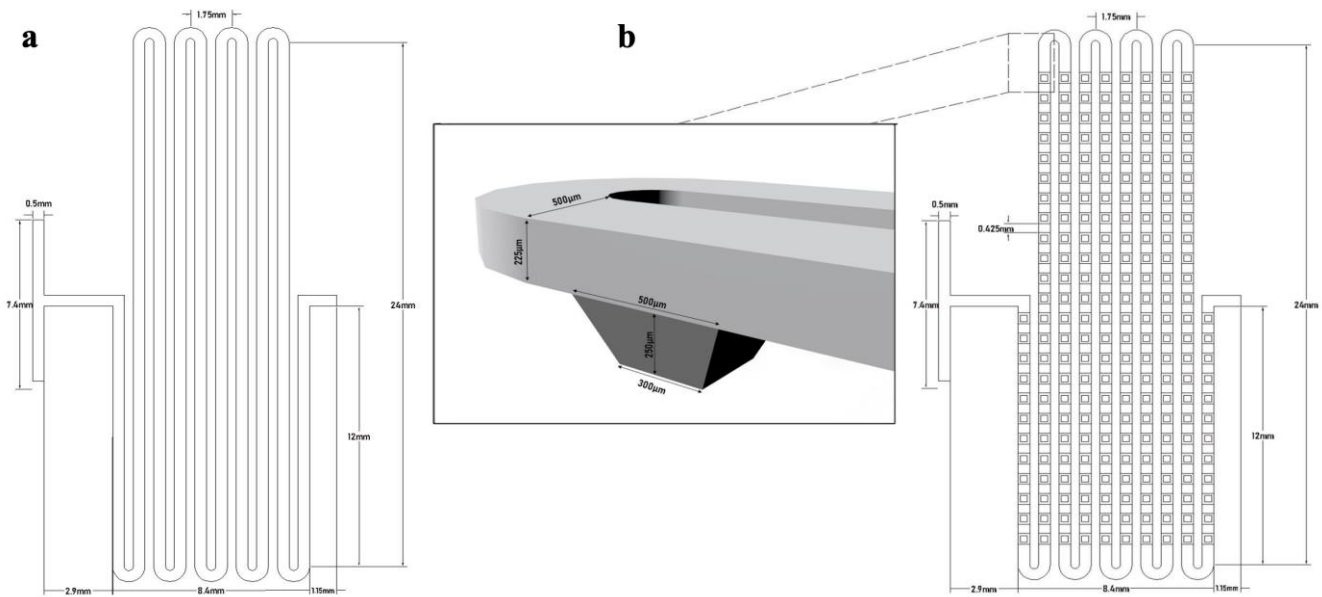


Figure 2. Micromixers dimensions and the channel configurations. a: Simple serpentine and b: Grooved serpentine microfluidic chips.

2.2. Numerical Modeling

To acquire the velocity profile inside the microchannel, the Navier-Stokes equations (conservation of momentum and continuity equations 2.1 and 2.2) are solved numerically. It is assumed that the fluids (DI water and blue dye) are Newtonian and incompressible under a steady-state pressure driven flow as follows,

$$\rho \left(\frac{\partial \mathbf{u}}{\partial t} + (\mathbf{u} \cdot \nabla) \mathbf{u} \right) = -\nabla p + \mu \nabla^2 \mathbf{u} \quad (2.1)$$

$$\nabla \cdot \mathbf{u} = 0 \quad (2.2)$$

where ρ is the fluid density (kg/m^3), \mathbf{u} is the velocity vector (m/s), t is the time (s), p is the pressure (Pa), and μ is the fluid viscosity ($\text{Pa}\cdot\text{s}$). The values for the viscosity and density are set to those for water at room temperature, i.e., $\mu = 1 \text{ mPa}\cdot\text{s}$ and $\rho = 1000 \text{ kg/m}^3$. No-slip boundary conditions are assigned for the walls of the micromixers. A free tetrahedral mesh, with all mesh elements not greater than $\sim 10 \mu\text{m}^3$ in volume, is applied for the entire microchannel. Aftermath, the flow fields obtained are utilized in the concentration-diffusion equation to evaluate the distribution of the concentration, c , through the mixer:

$$\frac{\partial c}{\partial t} = D \nabla^2 c - \mathbf{u} \cdot \nabla c \quad (2.3)$$

where D is the diffusion constant. The diffusion constant is set to $2.9 \times 10^{-9} \text{ m}^2/\text{s}$, corresponding to the typical diffusivity range of most ions in aqueous solutions [29].

The molar concentration C is chosen to be $1 \text{ (mol/m}^3\text{)}$ at one of the inlets and $0 \text{ (mol/m}^3\text{)}$ at the opposite inlet. The computational package COMSOL Multiphysics 5.4 and its Laminar Flow/Transport of Diluted Species modules is used to solve this multi-physics problem.

2.3. Mixing Analysis

In order to quantitatively investigate the effect of the flow rate and grooves on mixing, mixing index (MI) is calculated based on the following equation [30]:

$$MI = 1 - \frac{\sqrt{\frac{1}{n} \sum (I_i - I_{avg})^2}}{I_{avg}} \quad (2.4)$$

where n is the total number of the pixels, I_i is the dye intensity of each point, and I_{av} is the average intensity.

2.4. Geometrical Design of the Micromixer

The dimensions of the serpentine micromixers used in this study are shown in Figure 2. The fluids to be mixed are pumped into the mixer through a T-shaped inlet structure. Both inlets have a square shape of the same size of $500 \times 225 \mu\text{m}^2$. The height of the main channels is $H = 225 \mu\text{m}$, while its width is $W = 500 \mu\text{m}$ for both the simple and grooved serpentes investigated. In the grooved serpentine micromixer, the grooves are of a trapezoidal shape where each column is composed of 25 grooves placed at the bottom with spacing of $425 \mu\text{m}$ with dimensions shown in Figure 2b.

2.5. Experimental Implementation

Deionized (DI) water and a dilute blue dye solution are considered as the working fluids, each with a density of 1000 kg/m^3 and a dynamic viscosity of $1 \text{ mPa}\cdot\text{s}$. The diffusion coefficient of $2.9 \times 10^{-9} \text{ m}^2/\text{s}$ is taken for the dye solution in water. The fluids were pumped into the channels, via the two inlets, using a syringe pump simultaneously through 1.2 mm Teflon tubing. Since the aim of this work is to investigate the effect of the grooved-serpentine on mixing efficiency at different flow rates, total flow rates of $1000, 2000, 4000$ and $5000 \text{ }\mu\text{l/hr}$ are selected. An inverted microscope integrated with a CCD camera are used to monitor the fluid flow and mixing inside the micromixers.

3. Results and Discussion

The present study aims to investigate the relationship between the mixing index, flow rate, and Reynolds number in simple and grooved serpentine models. Furthermore, an in-depth analysis of the fluid dynamics in both models is conducted, and the pressure drop relation with Reynolds number along with numerical tools is analyzed and discussed.

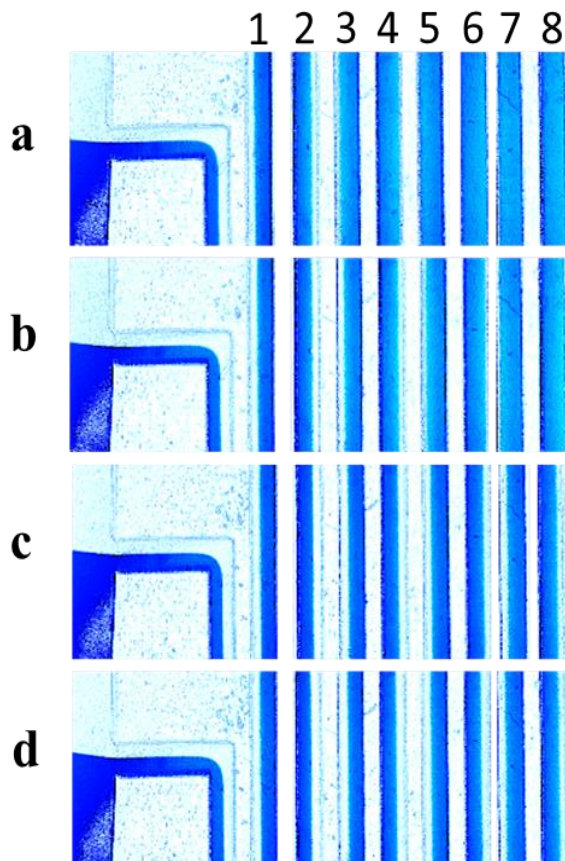


Figure 3. Experimental results of mixing performance at different locations in the simple serpentine channels under a: 1000 , b: 2000 , c: 4000 , and d: $5000 \text{ }\mu\text{l/hr}$.

3.1. Mixing Index vs Flow Rate

In the scope of this study, the effect of different flow rates on mixing efficiency is studied for two different serpentine models; simple serpentine and grooved serpentine. Total flow rates of $1000, 2000, 4000$ and $5000 \text{ }\mu\text{l/hr}$ are chosen to cover lower and higher flow rates. Figure 3 shows the experimental results of mixing along the middle region of the simple serpentine channel under four different flow rates.

From Figure 3, it is seen that the flow rate affects the mixing performance within the channel. As the flow rate increases, mixing efficiency of the blue dye and water is reduced. This is attributed to the phenomenon of strong flow symmetry in two streams (lacking disturbances in the flow to cause efficient mixing) and high shear force between them that is not enabling enough diffusion and mass transport of molecules [31]. At low flow rates, such as $1000 \text{ }\mu\text{l/hr}$, diffusion dominates the transport process and it plays a significant role in mixing, as the blue dye molecules are given enough time to diffuse across the channel and mix with the other stream of water. At such low flow rates, the fluid flows in smooth and parallel streamlines. However, as the flow rate increases ($2000, 4000$ and $5000 \text{ }\mu\text{l/hr}$), advection predominates over the molecular diffusion and controls the mass transport between the two fluids, which is a process by which substances/particles move from a high concentration region to a low concentration region until an equilibrium state is achieved [32]. This process carries the blue dye molecules along with the fluid stream without giving them enough time to diffuse across the channel and mix with the water. Thus, the fluids mix less efficiently and need high mixing length to observe efficient mixing.

Figure 4 shows the mixing index, calculated using Eq. (2.4), for the chosen four different flow rates at the exit of each column.

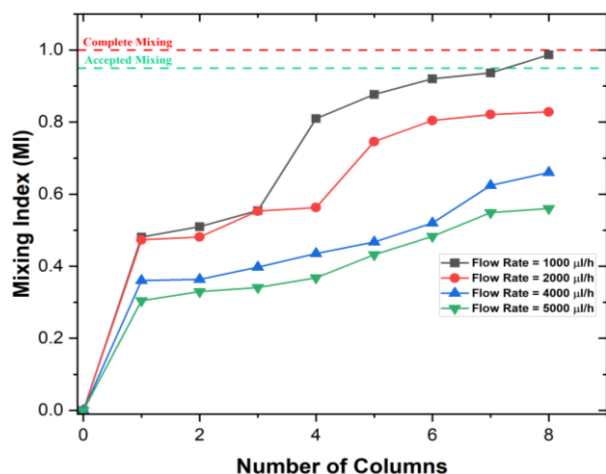


Figure 4. Mixing index along the simple serpentine channel for different flow rates.

In this study, a mixing index of 0.95 is taken a reference for an accepted mixing where a mixing index of 1.00 represents complete mixing and a mixing index of 0 represents no mixing at all. It is seen that for the case of 1000 $\mu\text{l/hr}$ flow rate only and after 8 turns, a mixing index of 0.98 is observed which is above the accepted mixing reference. However, for the other three flow rates, 2000, 4000 and 5000 $\mu\text{l/hr}$, the mixing index was observed to be much below the accepted mixing reference.

Next, experiments are carried out to investigate the effect of adding trapezoidal grooves to the bottom of the serpentine channel, named grooved serpentine, on the mixing performance at different flow rates. Figure 5 shows the experimental results of mixing along the middle of the grooved serpentine channel under four different flow rates. It is observed that mixing is achieved faster in the grooved serpentine as compared to the simple serpentine. Complete mixing is observed after the 3rd column (75 grooves) for the 1000 $\mu\text{l/hr}$ flow rate, whereas complete mixing is observed after the 8th column for the same flow rate in the simple serpentine model. Moreover, at higher flow rates (2000, 4000 and 5000 $\mu\text{l/hr}$), unlike in the simple serpentine case, complete mixing could be achieved within the same footprint. Thus, adding the grooves contributed to faster and enhanced mixing of the blue dye and DI water.

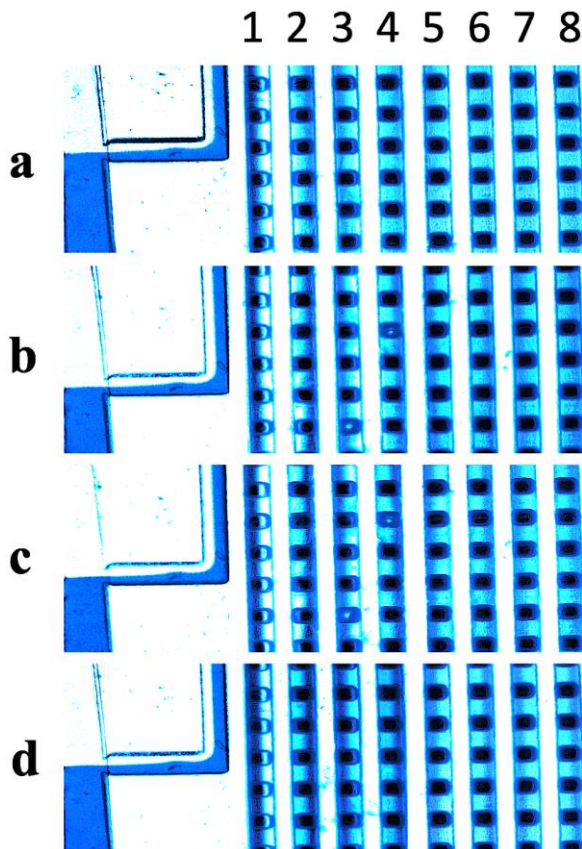


Figure 5. Experimental results of mixing performance at different locations in the grooved serpentine channels under a: 1000, b: 2000, c: 4000, and d: 5000 $\mu\text{l/hr}$.

To better understand the effect of adding the grooves on the mixing performance and efficiency, the mixing index at every column's exit for the four flow rates is calculated using Eq. (2.4) and shown in Figure 6.

It is seen that after 6 columns (150 grooves), complete mixing was observed for all the four flow rates. The trapezoidal grooves placed at the bottom of the serpentine channel cause repetitive, localized and periodic increase in the surface area of the channel that is available for mixing. In other words, the grooves disrupt the laminar flow regime as they act as a chain of baffles. The induced localized and periodic increase in the surface area within the channel significantly reduced the velocity stream in these regions due to localized pressure drops generated in those regions and break the symmetries in the flow and cause stirring effect.

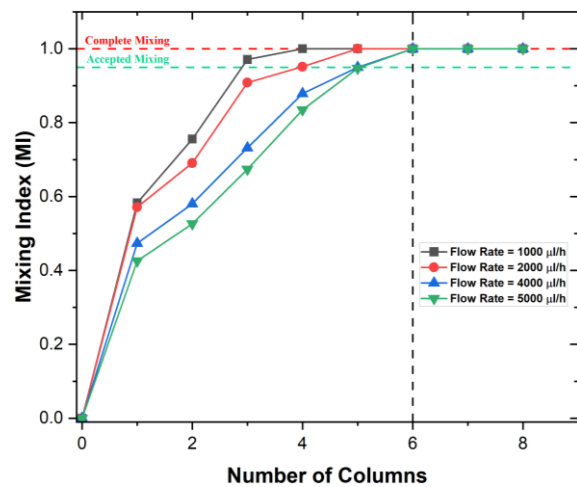


Figure 6. Mixing index along the grooved serpentine channel for different flow rates.

Figure 7 shows the velocity profile in both designs. The grooves enhanced convective transport of the fluid components along different parts of the microchannel due to the induced flow disruptions causing the fluids to be mixed more efficiently. Additionally, the trapezoidal grooves break-up the fluid flow into smaller segments by acting as micro-mixers cascaded through the grooved serpentine amplifying the mixing by each stage. Furthermore, the grooves cause the fluid to flow in a sinusoidal pattern, increasing the fluid-wall interaction as shown in Figure 8.

3.2. Mixing Index vs Reynolds Number

For the chosen flow rates, Reynolds number is calculated using:

$$Re = \frac{\rho u D_h}{\mu} \quad (3.1)$$

where Re is the Reynolds number, ρ is the fluid density (kg/m^3), u is the fluid velocity (m/s), D_h is the hydraulic diameter/characteristic length (m), and μ is the dynamic viscosity ($\text{Pa}\cdot\text{s}$) of the fluid.

Figure 9 shows the mixing index versus Reynolds number calculated at the inlet, mid-channel and outlet for the simple and grooved serpentine. The graph shows that at the outlet of the grooved serpentine, regardless of the Reynolds number value, the mixing index is 1 which represents complete mixing. However, at the outlet of the simple serpentine, as the Reynolds number increases, mixing index decreases which means that at higher Reynolds numbers and flow rates, the simple serpentine is not efficiently achieving acceptable mixing.

At low Reynolds numbers, molecules have enough interaction time to diffuse/move across the channel and mix with the other stream. This scenario is characterized by the predominance of diffusion in the transport process in which it plays a significant role in mixing [33]. At a Reynolds number higher than 1.2, the mixing index sharply decreases because the residence time decreases with increasing velocity and is insufficient for diffusion for the simple serpentine case. However, for the grooved serpentine case, staggered transversal vortices coupled with induced dean vortices, due to the centrifugal force exerted by the curvy structures of the serpentine, are fully effective in enhancing the mixing of fluids at such Reynolds number.

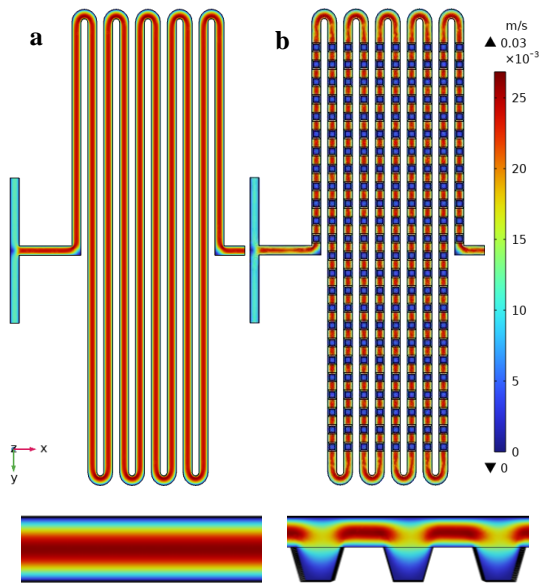


Figure 7. Velocity profile for 5000 µl/hr flow rate. a: Simple serpentine, b: Grooved serpentine channels.

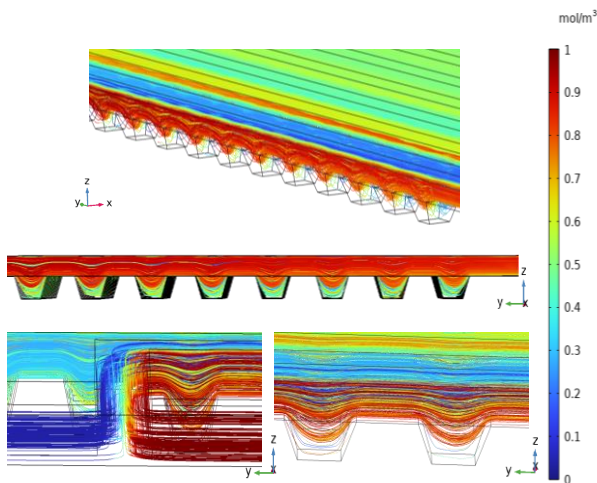


Figure 8. Concentration profile in the grooved serpentine channels.

The mixing index is high at Reynolds number of 1.2 despite strictly laminar flow and the absence of streamlines crossing because, at low flow rate, a long residence time of fluids in the channel allows more time for diffusion to occur, which is the dominant factor that causes mixing in this case.

3.3. Pressure Drop vs Reynolds Number

Reporting the pressure drop is an important factor to show the effect of the increasing the surface area within the channel due to the presence of grooves. Given that the pressure drop ($\Delta p = P_{in} - P_{out}$) is the pumping pressure needed at the inlet to drive the fluids through the channel. Figure 10 shows the pressure drop versus Reynolds number in both the simple and grooved serpentine.

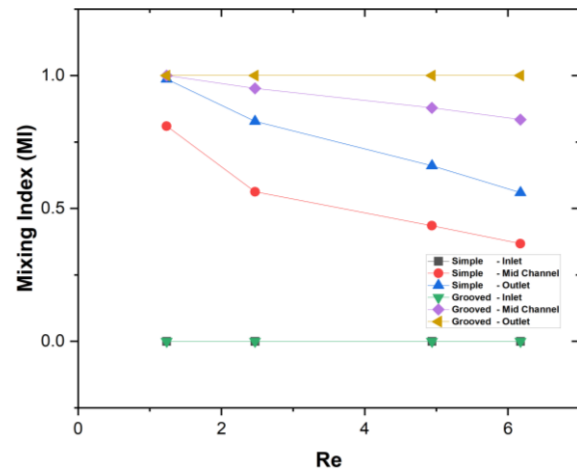


Figure 9. Mixing index vs Reynolds number.

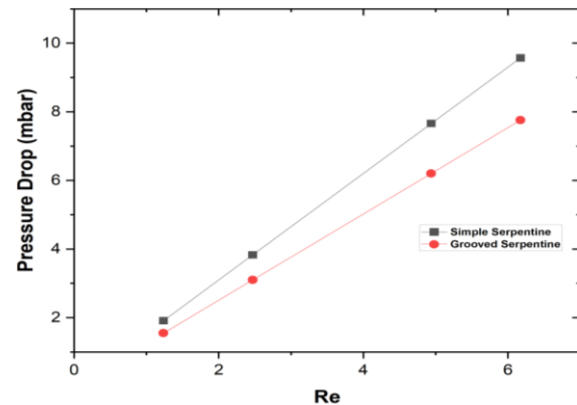


Figure 10. Pressure drop variation with the Reynolds number.

As seen in Figure 10, the grooved serpentine showed a lower relative pressure required to pump the fluids into the microchannel. By adding trapezoidal grooves to the bottom of the microfluidic channel, the effective surface area of the channel is increased, as the grooves provide additional surfaces for fluid-wall interactions; thus, forming localized pressure drops within the channel. For the same number of column and size of grooved serpentine and simple serpentine, mixing efficiency was greatly improved. Such design can be integrated in lab-on-a-chip systems with reduced footprint but with high mixing efficiency as simple serpentine would require much more serpentine channels to achieve acceptable mixing. By the use of the proposed grooved serpentine model, high mixing index for higher flow rates with low footprint and reduced complexity can be attained.

4. Conclusions

Numerical and experimental investigations were carried out to compare the mixing performance and efficiency of aqueous solutions of blue dye and water within a simple serpentine and grooved serpentine channel models. Results elucidated that the grooved serpentine microfluidic channels, consisting of trapezoidal-shaped structures aligned at the base of the main channel, showcased superlative mixing efficiencies, particularly at higher flow rates, as compared to the simple serpentine channels. The proposed grooved serpentine design enabled complete mixing of fluids, even at high flow rates, due to several factors: (1) localized increase of surface area at each groove, (2) localized pressure drops, (3) elongated fluid routes and thus longer fluid-fluid interaction time, (4) intensified fluid-wall interaction, and (5) coupled transversal and asymmetrical-induced flows which disrupted the laminar regime and velocity streamlines. This design holds a significant enhancement for microfluidic mixing systems due to its compact footprint and persistent high mixing efficiency. Future research could utilize such design to study mixing of higher viscous fluids.

Acknowledgement

Dr. Gurkan Yesiloz gratefully acknowledges the support from the Scientific and Technological Research Council of Türkiye (TUBITAK) (2232-Grant No: 118C263) and (1001-Grant No: 221M575). However, the entire responsibility of the publication/article belongs to the owner of the publication/article. The financial support received from TUBITAK does not mean that the content of the publication is approved in a scientific sense by TUBITAK.

Author's Contributions

Faruk Aksoy: Performed the experiments and analyzed the results.

Gurkan Yesiloz: Fabricated the chip, supervised the experimental progress, analyzed the structure of the work and the results. Both authors drafted and wrote the manuscript.

Ethics

There are no ethical issues after the publication of this manuscript.

References

- [1]. Sackmann, E.K.; Fulton, A.L.; Beebe, D.J. The present and future role of microfluidics in biomedical research. *Nature* 2014, 507, 181–189.
- [2]. Chiu, D.T.; deMello, A.J.; Di Carlo, D.; Doyle, P.S.; Hansen, C.; Maceiczky, R.M.; Wootton, R.C.R. Small but perfectly formed? Successes, challenges, and opportunities for microfluidics in the chemical and biological sciences. *Chem* 2017, 2, 201–223.
- [3]. Capretto, L.; Carugo, D.; Mazzitelli, S.; Nastruzzi, C.; Xunli, Z. Microfluidic and lab-on-a-chip preparation routes for organic nanoparticles and vesicular systems for nanomedicine applications. *Adv. Drug Deliv. Rev.* 2013, 65, 1496–1543.
- [4]. Khan, S.A.; Günther, A.; Schmidt, M.A.; Jensen, K.F. Microfluidic synthesis of colloidal silica. *Langmuir* 2004, 20, 8604–8611.
- [5]. Bamford, R.A.; Smith, A.; Metz, J.; Glover, G.; Titball, R.W.; Pagliara, S. Investigating the physiology of viable but non-culturable bacteria by microfluidics and time-lapse microscopy. *BMC Biol.* 2017, 15, 121.
- [6]. Jayamohan, H.; Sant, H.J.; Gale, B.K. Applications of microfluidics for molecular diagnostics. *Methods Mol. Biol.* 2013, 949, 305–334.
- [7]. Marasso, S.L.; Mombello, D.; Cocuzza, M.; Casalena, D.; Ferrante, I.; Nesca, A.; Poiklik, P.; Rekker, K.; Aaspollu, A.; Ferrero, S.; et al. A polymer lab-on-a-chip for genetic analysis using the arrayed primer extension on microarray chips. *Biomed. Microdevices* 2014, 16, 661–670.
- [8]. Zilionis, R.; Nainys, J.; Veres, A.; Savova, V.; Zemmour, D.; Klein, A.M.; Mazutis, L. Single-cell barcoding and sequencing using droplet microfluidics. *Nat. Protoc.* 2017, 12, 44–73.
- [9]. Makgwane, P.R.; Ray, S.S. Synthesis of nanomaterials by continuous-flow microfluidics: A review. *J Nanosci. Nanotech.* 2014, 14, 1338–1363.
- [10]. Lee, C.-Y.; Chang, C.-L.; Wang, Y.-N.; Fu, L.-M. Microfluidic mixing: a review. *Int. J. Mol. Sci.* 2011, 12, 3262–3287.
- [11]. Nguyen, N.-T. *Micromixers: Fundamentals, Design and Fabrication*, 2nd ed.; Elsevier: Oxford, UK, 2012; ISBN 978-1-4377-3520-8.
- [12]. Ward, K. and Fan, Z.H., 2015. Mixing in microfluidic devices and enhancement methods. *Journal of Micromechanics and Microengineering*, 25(9), p.094001.
- [13]. Wiggins, S.; Ottino, J.M. Foundations of chaotic mixing. *Philos. Trans. R. Soc. London Ser. A.* 2004, 362, 937–970.
- [14]. Lee, C.Y.; Wang, W.T.; Liu, C.C.; Fu, L.M. Passive mixers in microfluidic systems: A review. *Chem. Eng. J.* 2016, 288, 146–160.
- [15]. Buchegger, W.; Wagner, C.; Lendl, B.; Kraft, M.; Vellekoop, M.J. A highly uniform lamination micromixer with wedge shaped inlet channels for time resolved infrared spectroscopy. *Microfluid. Nanofluid.* 2011, 10, 889–897.
- [16]. Nimafar, M.; Viktorov, V.; Martinelli, M. Experimental comparative mixing performance of passive micromixers with H-shaped sub-channels. *Chem. Eng. Sci.* 2012, 76, 37–44.



- [17]. Lim, T.W.; Son, Y.; Jeong, Y.J.; Yang, D.-Y.; Kong, H.-J.; Lee, K.-S.; Kim, D.-P. Three-dimensionally crossing manifold micro-mixer for fast mixing in a short channel length. *Lab Chip* 2011, 11, 100–103.
- [18]. SadAbadi, H.; Packirisamy, M.; Wüthrich, R. High performance cascaded PDMS micromixer based on split-and-recombination flows for lab-on-a-chip applications. *RSC Adv.* 2013, 3, 7296.
- [19]. Kim, D.S.; Lee, S.H.; Kwon, T.H.; Ahn, C.H. A serpentine laminating micromixer combining splitting/recombination and advection. *Lab Chip* 2005, 5, 739–747.
- [20]. Rhoades, T., Kothapalli, C.R. and Fodor, P.S., 2020. Mixing optimization in grooved serpentine microchannels. *Micromachines*, 11(1), p.61.
- [21]. Javaid, M.U., Cheema, T.A. and Park, C.W., 2017. Analysis of passive mixing in a serpentine microchannel with sinusoidal side walls. *Micromachines*, 9(1), p.8.
- [22]. Mengeaud, V.; Josserand, J.; Girault, H.H. Mixing processes in a zigzag microchannel: Finite element simulations and optical study. *Anal. Chem.* 2002, 74, 4279–4286.
- [23]. Hossain, S.; Ansari, M.A.; Kim, K.Y. Evaluation of the mixing performance of three passive micromixers. *Chem. Eng. J.* 2009, 150, 492–501.
- [24]. Parsa, M.K.; Hormozi, F. Experimental and CFD modeling of fluid mixing in sinusoidal microchannels with different phase shift between side walls. *J. Micromech. Microeng.* 2014, 24, 65018.
- [25]. Parsa, M.K.; Hormozi, F.; Jafari, D. Mixing enhancement in a passive micromixer with convergent-divergent sinusoidal microchannels and different ratio of amplitude to wave length. *Comput. Fluids* 2014, 105, 82–90.
- [26]. Afzal, A.; Kim, K.Y. Convergent-divergent micromixer coupled with pulsatile flow. *Sens. Actuator B-Chem.* 2015, 211, 198–205.
- [27]. Akgönül, S.; Özbey, A.; Karimzadehkhoei, M.; Gozuacik, D.; Koşar, A. The effect of asymmetry on micromixing in curvilinear microchannels. *Microfluid. Nanofluid.* 2017, 21, 1–15.
- [28]. Liu, R.H.; Stremler, M.A.; Sharp, K.V.; Olsen, M.G.; Santiago, J.G.; Adrian, R.J.; Aref, H.; Beebe, D.J. Passive mixing in a three-dimensional serpentine microchannel. *J. Microelectromech. Syst.* 2000, 9, 190–197.
- [29]. Holz, M., Heil, S.R. and Sacco, A., 2000. Temperature-dependent self-diffusion coefficients of water and six selected molecular liquids for calibration in accurate 1H NMR PFG measurements. *Physical Chemistry Chemical Physics*, 2(20), pp.4740-4742.
- [30]. Yesiloz, G., Boybay, M.S. and Ren, C.L., 2017. Effective thermo-capillary mixing in droplet microfluidics integrated with a microwave heater. *Analytical Chemistry*, 89(3), pp.1978-1984.
- [31]. Stremler, M.A., Haselton, F.R. and Aref, H., 2004. Designing for chaos: applications of chaotic advection at the microscale. *Philosophical Transactions of the Royal Society of London. Series A: Mathematical, Physical and Engineering Sciences*, 362(1818), pp.1019-1036.
- [32]. Bordbar, A., Taassob, A. and Kamali, R., 2018. Diffusion and convection mixing of non-Newtonian liquids in an optimized micromixer. *The Canadian Journal of Chemical Engineering*, 96(8), pp.1829-1836.
- [33]. Cho, C.C., 2008. A combined active/passive scheme for enhancing the mixing efficiency of microfluidic devices. *Chemical Engineering Science*, 63(12), pp.3081-3087.